JOURNAL OF GUIDANCE, CONTROL, AND DYNAMICS
Vol. 33, No. 4, July–August 2010

Minimum-Landing-Error Powered-Descent Guidance for Mars Landing Using Convex Optimization

Lars Blackmore,* Behçet Açikmeşe,† and Daniel P. Scharf‡
Jet Propulsion Laboratory, California Institute of Technology, Pasadena, California 91109

DOI: 10.2514/1.47202

To increase the science return of future missions to Mars and to enable sample return missions, the accuracy with which a lander can be delivered to the Martian surface must be improved by orders of magnitude. The prior work developed a convex-optimization-based minimum-fuel powered-descent guidance algorithm. In this paper, this convex-optimization-based approach is extended to handle the case when no feasible trajectory to the target exists. In this case, the objective is to generate the minimum-landing-error trajectory, which is the trajectory that minimizes the distance to the prescribed target while using the available fuel optimally. This problem is inherently a nonconvex optimal control problem due to a nonzero lower bound on the magnitude of the feasible thrust vector. It is first proven that an optimal solution of a convex relaxation of the problem is also optimal for the original nonconvex problem, which is referred to as a lossless convexification of the original nonconvex problem. Then it is shown that the minimum-landing-error trajectory generation problem can be posed as a convex optimization problem and solved to global optimality with known bounds on convergence time. This makes the approach amenable to onboard implementation for real-time applications.

Nomenclature

$\mathbf{c}$	=	vector component of cone constraint
D	=	constraint on distance-to-target in horizontal plane
$\mathbf{e}$	=	unit vector normal to vector component of glide-slope constraint
$\mathbf{e}_i$	=	vector of zeros with unity at index i
$\mathbf{g}$	=	constant acceleration due to gravity
$H(\cdot)$	=	Hamiltonian
$h(\cdot)$	=	function defining glide-slope constraint
$J(t_f)$	=	cost for minimum-landing-error guidance problem
M	=	number of basis functions
$m(t)$	=	lander mass
m_{dry}	=	dry mass of lander
m_{wet}	=	wet mass of lander
N	=	number of discrete time steps
$\mathbf{p}_j$	=	basis function coefficient for control variables
$\mathbf{q}$	=	two-vector landing target in horizontal plane
$\mathbf{r}(t)$	=	position of lander
$\dot{\mathbf{r}}(t)$	=	velocity of lander
$\ddot{\mathbf{r}}(t)$	=	acceleration of lander
$\mathbf{r}_0$	=	initial position of lander
$\dot{\mathbf{r}}_0$	=	initial velocity of lander
S	=	matrix component of cone constraint
$\mathbf{T}_c(t)$	=	thrust profile
t	=	time
t_f	=	final time
t_k	=	time at kth time step
$\mathbf{u}(t)$	=	mass-normalized thrust profile
$\mathbf{X}$	=	set of allowed lander positions
$\mathbf{y}_k$	=	state at time t_k
$z(t)$	=	natural log of mass
$z_0(t)$	=	lower bound on natural log of mass
α	=	constant of proportionality between thrust magnitude and mass consumption
Γ	=	slack variable related to thrust magnitude
γ	=	glide-slope constraint angle
Δt	=	length of time step for discretization
ζ	=	normal to glide-slope constraint at contact point
μ	=	costate jump condition constant
Λ_k	=	matrix mapping constant disturbance to $\mathbf{y}_k$
λ	=	costate vector
ρ_1	=	lower bound on thrust magnitude
ρ_2	=	upper bound on thrust magnitude
$\sigma(t)$	=	mass-normalized thrust-magnitude slack variable
τ	=	time after contact with glide slope
Φ_k	=	discrete state transition matrix over k time steps
$\phi_j(t)$	=	basis function for control variables
Ψ_k	=	matrix mapping basis coefficients to $\mathbf{y}_k$
$\|\cdot\|$	=	two-norm of a vector

Received 15 September 2009; revision received 16 December 2009; accepted for publication 30 December 2009.

*Staff Engineer/Technologist, Guidance and Control Analysis Group, 4800 Oak Grove Drive, Mail Stop 198-326; lars@jpl.nasa.gov.

†Senior Engineer/Technologist, Guidance and Control Analysis Group, 4800 Oak Grove Drive, Mail Stop 198-326; behcet@jpl.nasa.gov. Senior Member AIAA (Corresponding Author).

‡Senior Engineer, Guidance and Control Engineer, Guidance and Control Analysis Group, 4800 Oak Grove Drive, Mail Stop 198-326; daniel.p.scharf@jpl.nasa.gov. Senior Member AIAA.

I. Introduction

THE science return of previous missions to the surface of Mars has been limited by the accuracy with which a lander can be delivered to the surface. Landing accuracy is characterized by the 3-sigma *landing ellipse*, which defines the region around the target in which landing can be guaranteed. The size of this ellipse (major axis) was approximately 150 km for Mars Pathfinder [1] and 35 km for the Mars Exploration Rovers [2]. The 2009 Mars Science Laboratory mission aims to achieve a landing ellipse of around 10 km [3]. This means that landing site selection is driven by the need to find a safe landing site, rather than by science goals. In other words, landing sites must be large, flat, and relatively rock- and crater-free areas to ensure safe landing [4]. These regions are usually not the sites with the maximum science return. For example, in the recent Phoenix mission, orbital images taken months before the landing showed a higher-than-expected concentration of large rocks at the primary landing site. This required a switch to an alternate landing site, which may not have been necessary if a more accurate landing were possible.

Recent work has focused on achieving pinpoint landing, which is defined as landing to within hundreds of meters of a target [5]. The pinpoint landing concept consists of an entry phase through the Martian atmosphere, followed by parachute deployment. During the parachute phase, errors accumulate due to winds and atmospheric uncertainty. Once the parachute is released, the final powered-descent phase then uses thrusters to land safely at the target. To do so, the lander needs to calculate onboard a trajectory from its a priori unknown location at parachute cutoff to the target. This powered-descent guidance (PDG) problem is challenging for a number of reasons. First, we must guarantee that any feasible solution obeys hard constraints, including minimum and maximum thrust magnitudes and a minimum glide-slope angle. The latter constraint also prevents subsurface flight. Second, we must guarantee that if a feasible solution exists, it will be found in a matter of seconds. This requirement is derived from the duration of the parachute and PDG phases; if the PDG algorithm takes too long to find a feasible solution, the lander can crash into the surface. The algorithm should find a globally optimal solution to maximize the distance from which the lander can reach the target given the amount of onboard fuel. Global optimality means that the system capability is limited only by the physical design of the spacecraft. By contrast, a PDG algorithm that finds only suboptimal or locally optimal solutions does not achieve the full retargeting range of the spacecraft.

A great deal of prior work has developed approximate solutions to the powered-descent guidance problem, including [3,6–12]. One of these is our convex optimization approach [3], which poses the problem of minimum-fuel powered-descent guidance as a second-order cone program (SOCP). This optimization problem can be solved in polynomial time using existing *interior-point-method* algorithms [13–15] that have a deterministic stopping criterion given a prescribed level of accuracy. That is, the global optimum can be computed to any given accuracy with an a priori known upper bound on the number of iterations required for convergence. In addition, interior-point-method algorithms of SOCPs are guaranteed to find a feasible solution if one exists [16]. This is in contrast with other approaches that either compute a closed-form solution by ignoring the constraints of the problem [8,17], propose solving a nonlinear optimization onboard [9,10], or solve a related problem that does not minimize fuel use [11]. The closed-form solution approach results in solutions that do not obey the constraints inherent in the problem, such as no subsurface flight constraints. This means that constraints must be checked explicitly after a solution is generated, and any solution that violates the constraints is rejected. In practice, this reduces the size of the region from which return to the target is possible by a factor of 10 or more [18]. Nonlinear optimization approaches, on the other hand, cannot provide a priori guarantees on how many iterations will be required to find a feasible trajectory and are not guaranteed to find the global optimum. This limits their relevance to onboard applications. For more extensive comparisons of the convex optimization approach to alternative approaches, see [12,18].

In this paper, we extend the convex optimization approach of [3] to handle the case when no feasible trajectory to the target exists. If no feasible trajectory to the target exists, the onboard guidance algorithm must ensure that a safe landing occurs as close as possible to the original target, if necessary, using all of the fuel available for powered-descent guidance. In this paper, we present an algorithm that solves this *minimum-landing-error* problem, which we define formally in Problem 3. The algorithm calculates the minimum-fuel trajectory to the target if one exists and calculates the trajectory that minimizes the landing error if no solution to the target exists. In the spirit of [3], our new approach poses the problem as two second-order cone programs, which can be solved to global optimality with known bounds on the number of iterations required. This minimum-landing-error capability will be necessary for missions that want to increase landing accuracy but cannot carry enough fuel to ensure that the target can be reached in all possible scenarios. The capability could also be used as a backup solution for missions that intend to land at a specified target but encounter offnominal conditions that prevent this from being possible.

The key difficulty in posing the minimum-landing-error problem as a convex optimization problem is the presence of nonconvex constraints: namely, the nonlinear system dynamics and the nonconvex thrust constraints. The thrust constraints are nonconvex because of a minimum-thrust-magnitude constraint, which arises because, once started, the thrusters cannot be throttled below a certain level. In [3], we rendered the minimum-fuel guidance problem convex by relaxing the nonconvex constraints and then proving that any optimal solution of the relaxed problem is also an optimal solution to the full nonconvex problem. We refer to this approach as lossless convexification. The primary theoretic contribution of the present paper is an analogous convexification for the minimum-landing-error powered-descent guidance problem. We pose two optimization problems in which the nonconvex constraints have been relaxed to yield second-order cone programs. We solve these problems sequentially and then provide a new analytic result that shows that any optimal solution to the second relaxed problem is also an optimal solution to the nonconvex minimum-landing-error problem. Furthermore, we show that the solution uses the least fuel of all the optimal solutions to the minimum-landing-error problem.

This paper is organized as follows: In Sec. II we review the convex optimization approach of [3] to solving the minimum-fuel PDG problem before defining the minimum-landing-error PDG problem in Sec. III. In Sec. IV we present the new algorithm for minimum-landing-error PDG, then present the main analytic result of the paper: namely, the convexification of nonconvex control constraints. Section V gives simulation results and Sec. VI presents our conclusions.

II. Review of Minimum-Fuel Powered-Descent Guidance

The minimum-fuel PDG problem consists of finding the thrust profile $\mathbf{T}_c(\cdot)$ that takes the lander from an initial position $\mathbf{r}_0$ and an initial velocity $\dot{\mathbf{r}}_0$ to rest at the prescribed target location, while minimizing the fuel mass consumed in doing so. The minimum-fuel PDG problem is defined formally in Problem 1. Throughout this paper we use $\mathbf{e}_i$ to denote a column vector of all zeros except the ith row, which is unity. We use $\|\mathbf{x}\|$ to denote the two-norm of the vector $\mathbf{x}$. We define the vertical (surface normal) direction to be along the vector $\mathbf{e}_1$ and let $\mathbf{g}$ be the constant acceleration vector due to gravity.

Problem 1 (nonconvex minimum-fuel guidance problem).

$$\max_{t_f,\mathbf{T}_c(\cdot)} m(t_f) - m(0) = \min_{t_f,\mathbf{T}_c(\cdot)} \int_0^{t_f} \alpha\|\mathbf{T}_c(t)\|\,\mathrm{d}t \tag{1}$$

subject to

$$\ddot{\mathbf{r}}(t) = \mathbf{g} + \mathbf{T}_c(t)/m(t) \qquad \dot{m}(t) = -\alpha\|\mathbf{T}_c(t)\| \tag{2}$$

$$0 < \rho_1 \le \|\mathbf{T}_c(t)\| \le \rho_2 \tag{3}$$

$$\mathbf{r}(t) \in \mathbf{X} \quad \forall\ t \in [0, t_f] \tag{4}$$

$$m(0) = m_{\text{wet}}, \qquad m(t_f) \ge m_{\text{dry}} \tag{5}$$

$$\mathbf{r}(0) = \mathbf{r}_0, \qquad \dot{\mathbf{r}}(0) = \dot{\mathbf{r}}_0 \tag{6}$$

$$\mathbf{e}_1^T\mathbf{r}(t_f) = 0, \qquad [\,\mathbf{e}_2 \quad \mathbf{e}_3\,]^T\mathbf{r}(t_f) = \mathbf{q}, \qquad \dot{\mathbf{r}}(t_f) = \mathbf{0} \tag{7}$$

where $\mathbf{q} \in \mathbb{R}^2$ defines the location of the landing target on the surface. We use $\mathbf{X}$ to define the set of feasible positions of the spacecraft: namely, the *glide-slope constraint*,

$$\mathbf{X} = \{\mathbf{r} \in \mathbb{R}^3 \colon \|S(\mathbf{r} - \mathbf{r}(t_f))\| - \mathbf{c}^T(\mathbf{r} - \mathbf{r}(t_f)) \le 0\} \tag{8}$$

where S and $\mathbf{c}$ are defined by the user to specify a feasible cone with a vertex at $\mathbf{r}(t_f)$:

$$S \triangleq \begin{bmatrix} 0 & 1 & 0 \\ 0 & 0 & 1 \end{bmatrix} \qquad \mathbf{c} \triangleq \frac{\mathbf{e}_1}{\tan\gamma}\gamma > 0 \tag{9}$$

Here, γ is the minimum glide-slope angle, illustrated in Fig. 1. The glide-slope constraint (8) ensures that the trajectory to the target cannot be too shallow and cannot go subsurface. $\mathbf{X}$ is a convex set and, for completeness, we give the standard definition of the interior of $\mathbf{X}$:

$$\text{int}\,\mathbf{X} \triangleq \{x \in \mathbf{X}: \exists\, \varepsilon > 0 \quad \text{such that } y \in \mathbf{X} \quad \text{if } \|x - y\| < \varepsilon\} \tag{10}$$

The boundary of $\mathbf{X}$ is given by $\partial\mathbf{X} \triangleq \{x \in \mathbf{X}: x \notin \text{int}\mathbf{X}\}$.

Equation (5) defines the initial mass of the lander and ensures that no more fuel is used than is available. Equation (6) defines the initial position and velocity of the lander, and Eq. (7) constrains the lander to be at rest at the target at the final time. Note also that the time of flight t_f is not fixed a priori, but is an optimization variable.

A key challenge in solving Problem 1 is the lower bound on the thrust magnitude in Eq. (3), which means that the set of allowable thrust values is nonconvex. This nonconvex control constraint prevents the direct use of convex optimization techniques in solving this problem. The key theoretical innovations of [3] are to relax these nonconvex constraints to give the following problem and to show that the optimal solution of this relaxed problem is also an optimal solution of Problem 1.

Problem 2 (relaxed minimum-fuel guidance problem).

$$\min_{t_f, \mathbf{T}_c(\cdot), \Gamma(\cdot)} \int_0^{t_f} \Gamma(t)\,\mathrm{d}t \tag{11}$$

subject to

$$\ddot{\mathbf{r}}(t) = \mathbf{g} + \mathbf{T}_c(t)/m(t) \qquad \dot{m}(t) = -\alpha\Gamma(t) \tag{12}$$

$$\|\mathbf{T}_c(t)\| \le \Gamma(t) \qquad 0 < \rho_1 \le \Gamma(t) \le \rho_2 \tag{13}$$

$$\mathbf{r}\,(t) \in \mathbf{X} \quad \forall\ t \in [0, t_f] \tag{14}$$

$$m(0) = m_{\text{wet}}, \qquad m(t_f) \ge m_{\text{dry}} \tag{15}$$

$$\mathbf{r}\,(0) = \mathbf{r}_0, \qquad \dot{\mathbf{r}}(0) = \dot{\mathbf{r}}_0 \tag{16}$$

$$\mathbf{e}_1^T\mathbf{r}(t_f) = 0, \qquad [\,\mathbf{e}_2 \quad \mathbf{e}_3\,]^T\mathbf{r}(t_f) = \mathbf{q}, \qquad \dot{\mathbf{r}}(t_f) = \mathbf{0} \tag{17}$$

Note that the nonconvex thrust constraints in Eq. (3) have been replaced with convex set of constraints (13). In [3] we showed that this constraint relaxation allows the discrete-time form of Problem 2 to be posed as a convex optimization problem. Furthermore, the following lemma formally states that an optimal solution to the relaxed minimum-fuel problem is also an optimal solution to the full nonconvex minimum-fuel PDG problem.

Lemma 1. Let $\{t_f^*, T_c^*(\cdot), \Gamma^*(\cdot)\}$ be an optimal solution to Problem 2 such that the corresponding state trajectory $\mathbf{r}^*(t)$ is on the boundary of the state constraints $\partial\mathbf{X}$ for, at most, one point $t \in (0, t_f^*)$.[§] Then $\{t_f^*, T_c^*(\cdot)\}$ is an optimal solution to Problem 1.

Proof: See the Appendix. □

The approach of [3] solves the nonconvex minimum-fuel PDG problem by solving a relaxed convex version of the problem. The convexification is *lossless*, in the sense that no part of the feasible space of the original problem is removed in the convexification process. The resulting optimization problem is a second-order cone program, for which solution techniques exist that guarantee the globally optimal solution can be found to a certain accuracy within a deterministic number of iterations. However, if a feasible solution does not exist, the optimization will simply report "infeasible," even though it may still be possible to land safely at some distance from the original target. In the next sections, therefore, we extend the approach of [3] to solve the minimum-landing-error problem.

[§]The state trajectory is on the boundary for, at most, one point if the trajectory either does not touch the boundary at all or touches the boundary instantaneously only once and does not remain on the boundary for a finite period of time.

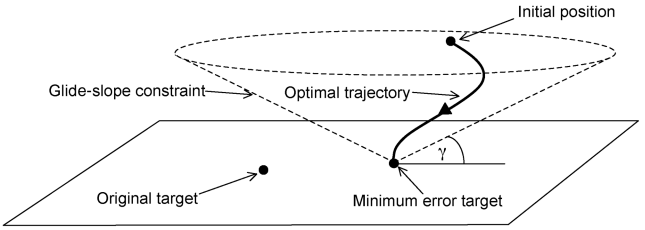

Fig. 1 Glide-slope constraint in minimum-landing-error powered-descent guidance problem. The glide-slope constraint requires the spacecraft to remain in a cone defined by the minimum slope angle γ. In the minimum-landing-error case, the apex of the cone coincides with the landed position of the spacecraft, rather than the original target.

III. Minimum-Landing-Error PDG Problem Statement

The minimum-landing-error powered-descent guidance problem consists of minimizing the final distance from the target subject to nonconvex thrust-magnitude constraints and glide-slope constraints, while ensuring that no more fuel mass is used than is available. The problem is stated formally in Problem 3.

Problem 3 (nonconvex minimum-landing-error guidance problem).

$$\min_{t_f, \mathbf{T}_c(\cdot)} \|\mathbf{r}(t_f)\|^2 \tag{18}$$

subject to

$$\ddot{\mathbf{r}}(t) = \mathbf{g} + \mathbf{T}_c(t)/m(t) \qquad \dot{m}(t) = -\alpha\|\mathbf{T}_c(t)\| \tag{19}$$

$$0 < \rho_1 \le \|\mathbf{T}_c(t)\| \le \rho_2 \tag{20}$$

$$\mathbf{r}\,(t) \in \mathbf{X} \quad \forall\ t \in [0, t_f] \tag{21}$$

$$m(0) = m_{\text{wet}}, \qquad m(t_f) \ge m_{\text{dry}} \tag{22}$$

$$\mathbf{r}\,(0) = \mathbf{r}_0, \qquad \dot{\mathbf{r}}(0) = \dot{\mathbf{r}}_0 \tag{23}$$

$$\mathbf{r}\,(t_f)^T\mathbf{e}_1 = 0, \qquad \dot{\mathbf{r}}(t_f) = \mathbf{0} \tag{24}$$

There are a number of key differences between this and the minimum-fuel guidance problem (Problem 1). First, the cost in Problem 3 is now the squared Euclidean distance from the target at the final time. Minimizing the squared distance is equivalent to minimizing the distance itself, since $\|\mathbf{r}(t_f)\| \ge 0$ and x^2 is monotonic for $x \ge 0$. To simplify notation we have assumed that the target is at zero, without loss of generality. Second, the final position is no longer required to be at the goal as in Eq. (7). Instead, Eq. (24) constrains the final altitude to be zero and the final velocity to be zero. Note that the cone constraints in Eq. (8) are defined around the state at the final time step and not around the origin. This definition allows a glide-slope constraint to be imposed even in the case that it is not possible to reach the target, as illustrated in Fig. 1.

Once again, the key difficulty in solving Problem 3 is that the thrust constraints (20) are nonconvex. The approach of [3] suggests that we overcome this problem through a similar convexification of the thrust

constraints. Unfortunately, the result in Lemma 1 does not apply to Problem 3. This means that we are not guaranteed that an optimal solution to a convexified relaxation of the minimum-landing-error problem is an optimal solution to the minimum-landing-error problem. In Sec. IV we therefore propose a new convexification for minimum-landing-error powered-descent guidance.

IV. Minimum-Landing-Error Powered-Descent Guidance Algorithm

A. Algorithm Description

In this section, we describe the main algorithm for the solution of the minimum-landing-error powered-descent problem (Problem 3). The key idea is to perform a prioritized optimization such that first, the distance between the prescribed target and the achievable landing location is minimized by solving Problem 4. Then a minimum-fuel trajectory achieving this minimum-landing-error is generated by solving Problem 5. This approach ensures that the resulting trajectory satisfies nonconvex thrust constraints and returns the globally optimal solution to Problem 3 if one exists. The new algorithm is given in Algorithm 1.

Problem 4 (relaxed minimum-landing-error guidance problem).

$$\min_{t_f,\mathbf{T}_c(\cdot),\Gamma(\cdot)} \|\mathbf{r}(t_f)\|^2 \tag{25}$$

subject to

$$\ddot{\mathbf{r}}(t) = \mathbf{g} + \mathbf{T}_c(t)/m(t) \qquad \dot{m}(t) = -\alpha\Gamma(t) \tag{26}$$

$$\|\mathbf{T}_c(t)\| \le \Gamma(t) \qquad 0 < \rho_1 \le \Gamma(t) \le \rho_2 \tag{27}$$

$$\mathbf{r}(t) \in \mathbf{X} \quad \forall\ t \in [0, t_f] \tag{28}$$

$$m(0) = m_{\text{wet}}, \qquad m(t_f) \ge m_{\text{dry}} \tag{29}$$

$$\mathbf{r}(0) = \mathbf{r}_0, \qquad \dot{\mathbf{r}}(0) = \dot{\mathbf{r}}_0 \tag{30}$$

$$\mathbf{r}(t_f)^T\mathbf{e}_1 = 0, \qquad \dot{\mathbf{r}}(t_f) = \mathbf{0} \tag{31}$$

Problem 5 (relaxed minimum-fuel guidance problem to specified range).

$$\min_{t_f,\mathbf{T}_c(\cdot),\Gamma(\cdot)} \int_0^{t_f} \Gamma(t)\,\mathrm{d}t \tag{32}$$

subject to

$$\ddot{\mathbf{r}}(t) = \mathbf{g} + \mathbf{T}_c(t)/m(t) \qquad \dot{m}(t) = -\alpha\Gamma(t) \tag{33}$$

$$\|\mathbf{T}_c(t)\| \le \Gamma(t) \qquad 0 < \rho_1 \le \Gamma(t) \le \rho_2 \tag{34}$$

$$\mathbf{r}(t) \in \mathbf{X} \quad \forall\ t \in [0, t_f] \tag{35}$$

$$m(0) = m_{\text{wet}}, \qquad m(t_f) \ge m_{\text{dry}} \tag{36}$$

Algorithm 1 Prioritized powered-descent guidance algorithm

1) Solve the relaxed minimum-landing-error guidance problem (Problem 4) for $\{t_f^*, T_c^*(\cdot), \Gamma^*(\cdot)\}$ with corresponding trajectory $\mathbf{r}^*(\cdot)$. If no solution exists, return `infeasible`.
2) Solve the relaxed minimum-fuel guidance problem to specified range (Problem 5) with $D = \|\mathbf{r}(t_f^*)\|$ for $\{t_f^\dagger, T_c^\dagger(\cdot), \Gamma^\dagger(\cdot)\}$.
3) Return $\{t_f^\dagger, T_c^\dagger(\cdot)\}$.

$$\mathbf{r}(0) = \mathbf{r}_0, \qquad \dot{\mathbf{r}}(0) = \dot{\mathbf{r}}_0 \tag{37}$$

$$\mathbf{r}(t_f)^T\mathbf{e}_1 = 0, \qquad \|\mathbf{r}(t_f)\| \le D, \qquad \dot{\mathbf{r}}(t_f) = \mathbf{0} \tag{38}$$

To generate Problem 4 we relaxed the nonconvex thrust constraints of the original minimum-landing-error problem stated in Problem 3. This relaxation is performed in the same manner that the minimum-fuel PDG problem is relaxed from Problem 1 to Problem 2. Since the relaxed minimum-landing-error problem (Problem 4) has convex inequality constraints on the state as well as on the controls, it can be solved with existing solvers. However, unlike minimum-fuel PDG, in which an optimal solution to the relaxed Problem 2 is also an optimal feasible solution to Problem 1, an optimal solution to the relaxed minimum-landing-error problem (Problem 4) is not necessarily an optimal feasible solution to the original minimum-landing-error problem, Problem 3. This is because the convexification proof provided in [3] does not hold for the minimum-landing-error problem. In particular, since the cost is landing error rather than fuel, the structure of the Hamiltonian in the resulting optimal control problem is different. Hence, another step is needed to ensure that the nonconvex thrust constraints are satisfied. This step consists of solving Problem 5, which also has relaxed constraints. However, since Problem 5 minimizes fuel use, we can use the result of Lemma 1 to prove that the solution to Problem 5 will satisfy the nonconvex thrust constraints of Problem 3. We will show in Sec. IV.B that the solution to Problem 5 is the optimal solution to Problem 3 and that it uses the minimum possible fuel of all optimal solutions to Problem 3.

To solve Problems 4 and 5 in practice, three additional steps are required: first, a change of variables to remove the nonlinear (and hence nonconvex) dynamic constraints; second, a discretization in time; and third, a line search for the optimal time of flight t_f^*. For these steps, we use an identical approach to that in [3], which we review in Secs. IV.C–IV.E.

B. Analytic Convexification Results

In this section, we provide two necessary lemmas before proving the main convexification result, which is given in Theorem 1.

Lemma 2. Assume that an optimal solution to Problem 5 exists, which we denote as $\{t_f^5, T_c^5(\cdot), \Gamma^5(\cdot)\}$, which has the corresponding trajectory $\mathbf{r}^5(\cdot)$ that is on the boundary $\partial\mathbf{X}$ for, at most, one point $t \in (0, t_f^5)$. Then $\{t_f^5, T_c^5(\cdot)\}$ is a feasible solution to Problem 1 with $\mathbf{q} = [\,\mathbf{e}_2 \quad \mathbf{e}_3\,]^T\mathbf{r}^5(t_f^5)$.

Proof: We first claim that $\{t_f^5, T_c^5(\cdot), \Gamma^5(\cdot)\}$ is an optimal solution to Problem 2 with $\mathbf{q} = [\,\mathbf{e}_2 \quad \mathbf{e}_3\,]^T\mathbf{r}^5(t_f^5)$. The proof of this claim is by contradiction. Let us assume that there exists a solution $\{t_f^*, T_c^*(\cdot), \Gamma^*(\cdot)\}$ that satisfies the constraints of Problem 2 with $\mathbf{q} = [\,\mathbf{e}_2 \quad \mathbf{e}_3\,]^T\mathbf{r}^5(t_f^5)$ but that also has

$$\int_0^{t_f^*} \Gamma^*(t)\,\mathrm{d}t < \int_0^{t_f^5} \Gamma^*(t)\,\mathrm{d}t \tag{39}$$

Comparing constraints, we see that $\{t_f^*, T_c^*(\cdot), \Gamma^*(\cdot)\}$ is a feasible solution to Problem 5. Hence, $\{t_f^*, T_c^*(\cdot), \Gamma(\cdot)\}$ is a feasible solution with lower cost than the optimal solution $\{t_f^5, T_c^5(\cdot), \Gamma^5(\cdot)\}$, which leads to a contradiction. Hence, $\{t_f^5, T_c^5(\cdot), \Gamma^5(\cdot)\}$ is an optimal solution to Problem 2 with $\mathbf{q} = [\,\mathbf{e}_2 \quad \mathbf{e}_3\,]^T\mathbf{r}^5(t_f^5)$. Since $\mathbf{r}^5(t)$ is on the boundary $\partial\mathbf{X}$ for, at most, once in the interval $(0, t_f^5)$, then by Lemma 1, $\{t_f^5, T_c^5(\cdot)\}$ is a feasible solution to Problem 1 with $\mathbf{q} = [\,\mathbf{e}_2 \quad \mathbf{e}_3\,]^T\mathbf{r}^5(t_f^5)$.

Lemma 3. Assume that an optimal solution to Problem 4 exists, which we denote as $\{t_f^4, T_c^4(\cdot), \Gamma^4(\cdot)\}$ with corresponding trajectory $\mathbf{r}^4(\cdot)$. Then there exists a feasible optimal solution to Problem 5 with $D = \|\mathbf{r}^4(t_f^4)\|$, which we denote as $\{t_f^5, T_c^5(\cdot), \Gamma^5(\cdot)\}$ with corresponding trajectory $\mathbf{r}^5(\cdot)$. Assume further that this trajectory is on the boundary $\partial\mathbf{X}$ for, at most, one point $t \in (0, t_f^5)$. Then $\{t_f^5, T_c^5(\cdot)\}$ is a feasible optimal solution to Problem 3. Furthermore,

$\{t_f^5, T_c^5(\cdot)\}$ uses the minimum possible fuel of all optimal solutions to Problem 3.

Proof: First, note that $\{t_f^4, T_c^4(\cdot), \Gamma^4(\cdot)\}$ is a feasible solution to Problem 5 with $D = \|\mathbf{r}^4(t_f^4)\|$, since the only additional constraint in Problem 5 is $\|\mathbf{r}(t_f)\| \leq D$ and, by design, we have $D = \|\mathbf{r}^4(t_f^4)\|$. Hence, a feasible solution to Problem 5 exists for $D = \|\mathbf{r}^4(t_f^4)\|$. Solving this problem, we obtain $\{t_f^5, T_c^5(\cdot), \Gamma^5(\cdot)\}$, and from Lemma 2, we know that $\{t_f^5, T_c^5(\cdot)\}$ is a feasible solution to Problem 1 for $\mathbf{q} = [\,\mathbf{e}_2 \quad \mathbf{e}_3\,]^T \mathbf{r}^5(t_f^5)$. By comparing constraints, we see that any feasible solution to Problem 1 is a feasible solution to Problem 3. Hence, $\{t_f^5, T_c^5(\cdot)\}$ is a feasible solution to Problem 3. This means that

$$\|\mathbf{r}^5(t_f^5)\| \geq \|\mathbf{r}^3(t_f^3)\| \tag{40}$$

where $\mathbf{r}^3(\cdot)$ denotes the trajectory corresponding to the optimal solution to Problem 3. Since Problem 4 is a relaxation of Problem 3, we know that $\|\mathbf{r}^4(t_f^4)\| \leq \|\mathbf{r}^3(t_f^3)\|$. Since in Problem 5 we have assigned $D = \|\mathbf{r}^4(t_f^4)\|$, we also know that $\|\mathbf{r}^5(t_f^5)\| \leq \|\mathbf{r}^4(t_f^4)\|$, and hence

$$\|\mathbf{r}^5(t_f^5)\| \leq \|\mathbf{r}^3(t_f^3)\| \tag{41}$$

Combining Eqs. (40) and (41), we have $\|\mathbf{r}^5(t_f^5)\| = \|\mathbf{r}^3(t_f^3)\|$. Hence, the landing error in the optimal solution to Problem 5 is the same as that in a globally optimal solution to Problem 3. We have already shown that $\{t_f^5, T_c^5(\cdot)\}$ is a feasible solution to Problem 3. As a result, $\{t_f^5, T_c^5(\cdot)\}$ is an optimal solution to Problem 3.

We now show that $\{t_f^5, T_c^5(\cdot)\}$ uses the minimum possible fuel of all optimal solutions to Problem 3. We know that $\{t_f^5, T_c^5(\cdot)\}$ is an optimal solution to Problem 3. Therefore, all optimal solutions to Problem 3 have $\|\mathbf{r}(t_f)\| = \|\mathbf{r}^5(t_f^5)\| \leq \|\mathbf{r}^4(t_f^4)\|$. The proof is by contradiction. Assume that there exists an optimal solution $\{t_f^\dagger, T_c^\dagger(\cdot)\}$ to Problem 3 with corresponding trajectory $\mathbf{r}^\dagger(\cdot)$ that also has

$$\int_0^{t_f^\dagger} \|\mathbf{T}_c^\dagger(t)\|\,\mathrm{d}t < \int_0^{t_f^5} \|\mathbf{T}_c^5(t)\|\,\mathrm{d}t \tag{42}$$

Comparing constraints, since $\|\mathbf{r}^\dagger(t_f^\dagger)\| \leq \|\mathbf{r}^4(t_f^4)\|$, we know that $\{t_f^\dagger, T_c^\dagger(\cdot), \Gamma^\dagger(\cdot)\}$ with $\Gamma^\dagger(\cdot) = \|\mathbf{T}_c^\dagger(\cdot)\|$ is also a feasible solution to Problem 5 with $D = \|\mathbf{r}^4(t_f^4)\|$. From Eq. (42) this solution has lower cost than $\{t_f^5, T_c^5(\cdot)\}$. This leads to a contradiction, since $\{t_f^5, T_c^5(\cdot), \Gamma^5(\cdot)\}$ is the optimal solution to Problem 5 with $D = \|\mathbf{r}^4(t_f^4)\|$. Hence, there is no optimal solution to Problem 3 that uses less fuel than $\{t_f^5, T_c^5(\cdot)\}$ □.

The following theorem is the main result of this paper and it follows from Lemmas 1 through 3.

Theorem 1. If a solution to the nonconvex minimum-landing-error guidance problem (Problem 3) exists, then the prioritized powered-descent guidance algorithm returns a solution $\{t_f^\dagger, T_c^\dagger(\cdot)\}$ with trajectory $\mathbf{r}^\dagger(\cdot)$. If this trajectory is on the boundary of the state constraints $\partial\mathbf{X}$ for, at most, one point $t \in (0, t_f^\dagger)$, then it is an optimal solution to Problem 3. Furthermore, the returned solution uses the minimal fuel among all optimal solutions of Problem 3.

Proof: Since Problem 4 is a relaxation of Problem 3, we know that if there is a feasible solution to Problem 3, there exists a feasible solution to Problem 4, and the prioritized powered-descent guidance will not return `infeasible`. Then from Lemma 3 we know that $\{t_f^\dagger, T_c^\dagger(\cdot)\}$ is an optimal solution to Problem 3 and that this solution uses the least fuel of all optimal solutions to Problem 3. □

Note that Theorem 1 implies that the prioritized powered-descent guidance algorithm returns `infeasible` only if no solution to the nonconvex minimum-landing-error guidance problem (Problem 3) exists. Hence, the convexification approach is lossless, in the sense that no part of the feasible region of the original problem is removed by convexifying the nonconvex constraints.

Remark 1. As with the minimum-fuel powered-descent guidance problem, we have observed that for Mars landing, all the optimal trajectories that are generated via solving the relaxed minimum-fuel guidance problem to specified range touch the boundary of the feasible state region at one point, at most. Hence, the prioritized powered-descent guidance algorithm has always returned optimal solutions to the original nonconvex minimum-landing-error problem for Mars powered-descent guidance. This includes an extensive empirical investigation across the space of feasible initial conditions and system parameters.

Remark 2. Observe that in step 1 of the prioritized powered-descent guidance algorithm, we do not necessarily obtain a fuel-optimal solution, but step 2 ensures that a fuel-optimal solution is found. In this way, the two-step approach is a way of prioritizing a multi-objective optimization problem. This approach is different from the more typical regularization procedure in which both distance and fuel costs are combined in a single cost function to ensure that a single optimal solution exists. The prioritization approach removes two of the key problems associated with regularization. First, regularization requires that the relative weights on fuel and distance are chosen, which is usually carried out in an ad hoc manner. Second, regularized solutions do not necessarily make physical sense. Our approach removes this ambiguity from the problem description and obtains a physically meaningful solution.

C. Change of Variables

We use the following change of variables to remove the nonlinear state dynamics (26):

$$\sigma \triangleq \frac{\Gamma}{m} \qquad \mathbf{u} \triangleq \frac{\mathbf{T}_c}{m} \qquad z \triangleq \ell_n\, m \tag{43}$$

Equation (26) can then be rewritten as

$$\ddot{\mathbf{r}}(t) = \mathbf{u}(t) + \mathbf{g} \tag{44}$$

$$\dot{z} = \frac{\dot{m}(t)}{m(t)} = -\alpha\sigma(t) \tag{45}$$

The change of variables therefore yields a set of linear equations for the state dynamics. The control constraints, however, are no longer convex. These are now given by

$$\|\mathbf{u}(t)\| \leq \sigma(t) \quad \forall\ t \in [0, t_f] \tag{46}$$

$$\rho_1 e^{-z(t)} \leq \sigma(t) \leq \rho_2 e^{-z(t)} \quad \forall\ t \in [0, t_f] \tag{47}$$

As in [3], we use a second-order-cone approximation of the inequalities in Eq. (47) that can be readily incorporated into the SOCP solution framework, given by

$$\rho_1 e^{-z_0}\left[1 - (z(t) - z_0(t)) + \frac{(z(t) - z_0(t))^2}{2}\right] \leq \sigma(t) \leq \rho_2 e^{-z_0}[1 - (z(t) - z_0(t))] \quad \forall\ t \in [0, t_f] \tag{48}$$

where

$$z_0(t) = \ell_n(m_{\text{wet}} - \alpha\rho_2 t) \tag{49}$$

and m_{wet} is the initial mass of the spacecraft. An approximation of Problem 4 can now be expressed in terms of the new control variables:

Problem 6 (relaxed minimum-landing-error problem with changed variables).

$$\min_{t_f, \mathbf{T}_c(\cdot), \Gamma(\cdot)} \|\mathbf{r}(t_f)\|^2 \tag{50}$$

subject to

$$\ddot{\mathbf{r}}(t) = \mathbf{g} + \mathbf{u}(t) \qquad \dot{z}(t) = -\alpha\sigma(t) \tag{51}$$

$$\|\mathbf{u}(t)\| \leq \Gamma(t) \tag{52}$$

$$\rho_1 e^{-z_0(t)}\left[1-(z(t)-z_0(t))+\frac{(z(t)-z_0(t))^2}{2}\right] \le \sigma(t) \le \rho_2 e^{-z_0(t)}[1-(z(t)-z_0(t))] \tag{53}$$

$$\mathbf{r}(t) \in \mathbf{X} \quad \forall\ t \in [0, t_f] \tag{54}$$

$$m(0) = m_{\text{wet}}, \qquad m(t_f) \ge m_{\text{dry}} \tag{55}$$

$$\mathbf{r}(0) = \mathbf{r}_0, \qquad \dot{\mathbf{r}}(0) = \dot{\mathbf{r}}_0 \tag{56}$$

$$\mathbf{r}(t_f)^T \mathbf{e}_1 = 0, \qquad \dot{\mathbf{r}}(t_f) = \mathbf{0} \tag{57}$$

Problem 6 is an approximation of the relaxed minimum-landing-error PDG problem (Problem 4) in which the nonlinear equality constraints have been eliminated. Furthermore, [3] shows that the approximation of the inequalities in Eq. (47) given by Eq. (48) is generally very accurate for both parts of the inequality and derives an analytic upper bound on the approximation error.

D. Time Discretization

We now discretize Problem 6 to convert the infinite-dimensional optimization problem to a finite-dimensional one by discretizing the time domain into equal time intervals and imposing the constraints at edges of the time steps, which we refer to as temporal nodes. Since the constraints are linear or second-order-cone constraints, the resulting problem is a finite-dimensional SOCP problem that can be efficiently solved by readily available algorithms [13–15]. We use the same approach as in [3] and refer the reader to this paper for more details.

For any given time interval $[0, t_f]$ and time increment Δt, the temporal nodes are given as

$$t_k = k\Delta t \qquad k = 0, \ldots, N$$

where $N\Delta t = t_f$. Define a vector of parameters as

$$\eta = \begin{bmatrix} \mathbf{p}_0 \\ \vdots \\ \mathbf{p}_M \end{bmatrix} \tag{58}$$

where $\mathbf{p}_j \in \mathbb{R}^4$. We describe the control input $\mathbf{u}$ and σ in terms of these parameters and some prescribed basis functions $\phi_1(\cdot), \ldots, \phi_M(\cdot)$:

$$\begin{bmatrix} \mathbf{u}(t) \\ \sigma(t) \end{bmatrix} = \sum_{j=0}^{M} \mathbf{p}_j \phi_j(t) \qquad t \in [0, t_f] \tag{59}$$

Then the solution of the differential equations (44) and (45) at the temporal nodes and the control inputs at the temporal nodes can be expressed in terms of these coefficients:

$$\mathbf{y}_k \triangleq \begin{bmatrix} \mathbf{r}(t_k) \\ \dot{\mathbf{r}}(t_k) \\ z(t_k) \end{bmatrix} = \Phi_k \begin{bmatrix} \mathbf{r}_0 \\ \dot{\mathbf{r}}_0 \\ \ell_n\, m_{\text{wet}} \end{bmatrix} + \Lambda_k \begin{bmatrix} \mathbf{g} \\ 0 \end{bmatrix} + \Psi_k \eta \qquad k = 1, \ldots, N \tag{60}$$

$$\begin{bmatrix} \mathbf{u}_k \\ \sigma_k \end{bmatrix} \triangleq \begin{bmatrix} \mathbf{u}(t_k) \\ \sigma(t_k) \end{bmatrix} = \Upsilon_k \eta \qquad k = 1, \ldots, N \tag{61}$$

where Φ_k, Ψ_k, Λ_k, and Υ_k are matrix functions of the time index k determined by the basis functions chosen. In this paper, we use piecewise linear basis functions with $M = N$, such that

$$\phi_j(t) = \begin{cases} \frac{t_j - t}{\Delta t} & \text{when } t \in [t_{j-1}, t_j) \\ \frac{t - t_j}{\Delta t} & \text{when } t \in [t_j, t_{j+1}) \\ 0 & \text{otherwise} \end{cases} \tag{62}$$

This corresponds to first-order hold discretization of a linear time-invariant system for the dynamics of the spacecraft [Eqs. (44) and (45)], with the vector $[\mathbf{r}(t_k)^T,\ \dot{\mathbf{r}}(t_k)^T,\ z(t_k)^T]^T$ as the state. Explicit expressions for Φ_k, Ψ_k, Λ_k, and Υ_k can be obtained using standard techniques; we do not repeat this derivation here, but refer the interested reader to [19]. Now, with the following additional notation, Problem 7 describes the discretized version of Problem 6:

$$E = [I_{3\times3} \quad 0_{3\times4}] \qquad F = [0_{1\times6} \quad 1] \qquad E_{\mathbf{u}} = [I_{3\times3} \quad 0_{3\times1}]$$
$$E_{\mathbf{v}} = [0_{3\times3} \quad I_{3\times3} \quad 0_{3\times1}] \tag{63}$$

Problem 7 (discretized relaxed minimum-landing-error guidance problem).

$$\min_{N,\eta} \|E\mathbf{y}_N\|^2 \tag{64}$$

subject to

$$\|E_{\mathbf{u}} \Upsilon_k \eta\| \le \mathbf{e}_4^T \Upsilon_k \eta \qquad k = 0, \ldots, N \tag{65}$$

$$\rho_1 e^{-z_0(t_k)}\left[1-(F\mathbf{y}_k - z_0(t_k)) + \frac{(F\mathbf{y}_k - z_0(t_k))^2}{2}\right] \le \mathbf{e}_4^T \Upsilon_k \eta \le \rho_2 e^{-z_0(t_k)}[1-(F\mathbf{y}_k - z_0(t_k))] \tag{66}$$

$$E\mathbf{y}_k \in \mathbf{X} \qquad k = 1, \ldots, N \tag{67}$$

$$F\mathbf{y}_N \ge \ell_n\, m_{\text{dry}} \tag{68}$$

$$\mathbf{y}_N^T \mathbf{e}_1 = 0, \qquad E_{\mathbf{v}} \mathbf{y}_N^T = \mathbf{0} \tag{69}$$

$$\mathbf{y}_k = \Phi_k \begin{bmatrix} \mathbf{r}_0 \\ \dot{\mathbf{r}}_0 \\ \ell_n\, m_{\text{wet}} \end{bmatrix} + \Lambda_k \begin{bmatrix} \mathbf{g} \\ 0 \end{bmatrix} + \Psi_k \eta \qquad k = 1, \ldots, N \tag{70}$$

Note that for any given N, Problem 7 defines a finite-dimensional SOCP, which can be solved very efficiently with guaranteed convergence to the globally optimal solution by using existing SOCP algorithms [14,16,20]. Here, N describes the time of flight since $t_f = N\Delta t$. It remains to find the optimal time of flight, which we achieve using a line search.

E. Time-of-Flight Search

For minimum-fuel powered-descent guidance, [3] uses a line search to find the optimal time of flight t_f^*. In this section, we apply this approach to the minimum-landing-error guidance problem. Extending [3], [21] uses a golden search technique (page 726 in [22], which ensures that the interval in which the optimal value is known to lie shrinks by the same constant proportion at each iteration. The technique relies, however, on two key properties of $J(t_f)$: the optimal cost of Problem 3 as a function of t_f, that is,

$$J(t_f) = \min_{\mathbf{T}_c(\cdot),\Gamma(\cdot)} \|\mathbf{r}(t_f)\|^2 \tag{71}$$

subject to Eqs. (19–24). First, we must know an interval in which t_f^* is known to lie. That is, we must find bounds t_l and t_u such that $t_l \le t_f^* \le t_u$. Second, $J(t_f)$ must be unimodal (page 726 in [22] for a definition of unimodal functions).

In [21] the authors solve the one-dimensional powered-descent guidance problem using the approach of [6] to obtain values for t_l and t_u. In the case of minimum-landing-error guidance, we can use the

same approach to obtain t_l. The approach of [21] for obtaining t_u does not, however, extend to the minimum-landing-error case. Instead, we use a heuristic scaling to set $t_u = k_{\text{scale}} t_l$, where k_{scale} is on the order of 3. Then, assuming unimodality of $J(t_f)$, the golden search approach checks analytically whether t_u is a true upper bound. If not, t_u is increased until it is an upper bound on t_f^*.

In [21] the authors observed experimentally that $J(t_f)$ is indeed a unimodal function. Since the present paper is concerned with the minimum-landing-error problem, this conclusion does not carry over from the minimum-fuel case. In Sec. V.B we show experimentally that $J(t_f)$ is unimodal and that the golden search approach finds t_f^* to within a few percent.

V. Simulation Results

In this section, we present simulation results obtained using the new algorithm. The second-order-cone programs were solved using G-OPT, a Jet Propulsion Laboratory in-house convex optimizer. Simulations were run on a MacBook Pro 2.4 GHz with 4 GB RAM. In Sec. V.A we present some example solutions generated by the new approach, and in Sec. V.B we empirically demonstrate the unimodality of the optimal solution with respect to the time of flight.

A. Example Solutions

We first consider a case when the target can be reached given the available fuel, then a case when the target cannot be reached. The spacecraft parameters for these simulations are

$$\mathbf{g} = [-3.7114 \text{ m/s}^2 \quad 0 \quad 0]^T \qquad m_{\text{dry}} = 1505 \text{ kg}$$
$$m_{\text{wet}} = 1905 \text{ kg} \qquad \alpha = 4.53 \times 10^{-4} \text{ s/m} \qquad \rho_1 = 4972N$$
$$\rho_2 = 13260N \tag{72}$$

A glide-slope constraint is used to prevent the trajectory from descending at an angle shallower than 4°. The spacecraft initial position is given by

$$\mathbf{r}_0 = \begin{bmatrix} 1500 \text{ m} \\ 500 \text{ m} \\ 2000 \text{ m} \end{bmatrix} \tag{73}$$

In case 1, the initial velocity is denoted $\dot{\mathbf{r}}_0^{(1)}$ and is given by

$$\dot{\mathbf{r}}_0^{(1)} = \begin{bmatrix} -75 \text{ m/s} \\ 0 \\ 100 \text{ m/s} \end{bmatrix} \tag{74}$$

In Figs. 2 we show results generated for case 1 using the new prioritized minimum-landing-error PDG approach (Algorithm 1) with 55 time-discretization points. Golden search was terminated when the optimal time of flight was known to within an interval of 3.0 s. In this case, there exists a feasible trajectory to the target, so the algorithm returns the minimum-fuel solution to the target. This solution requires 399.4 kg of fuel and has $t_f^* = 78.4$ s. The total computation time required was 14.3 s, and 23 iterations of golden search were used. Note that almost all of the available fuel was required to reach the target. This example illustrates the value of the convex optimization, which guarantees finding a solution if one exists; even cases at the edge of the physical capabilities of the spacecraft can be solved.

In case 2, there is an additional initial velocity in the y direction:

$$\dot{\mathbf{r}}_0^{(2)} = \begin{bmatrix} -75 \text{ m/s} \\ 40 \text{ m/s} \\ 100 \text{ m/s} \end{bmatrix} \tag{75}$$

Since case 1 used almost all of the available fuel, and case 2 has an initial velocity in the y direction away from the target, it is most likely that there will be insufficient fuel to reach the target. We verify this by attempting to solve the minimum-fuel PDG problem using the algorithm of [3], which reports that the problem is infeasible and that at least 414 kg of fuel is required to reach the target. The minimum-landing-error targeting algorithm, however, finds a solution that ensures safe landing at a distance of 404 m from the target. The solution, shown in Fig. 3, has $t_f^* = 77.7$ s and uses the full 400 kg of

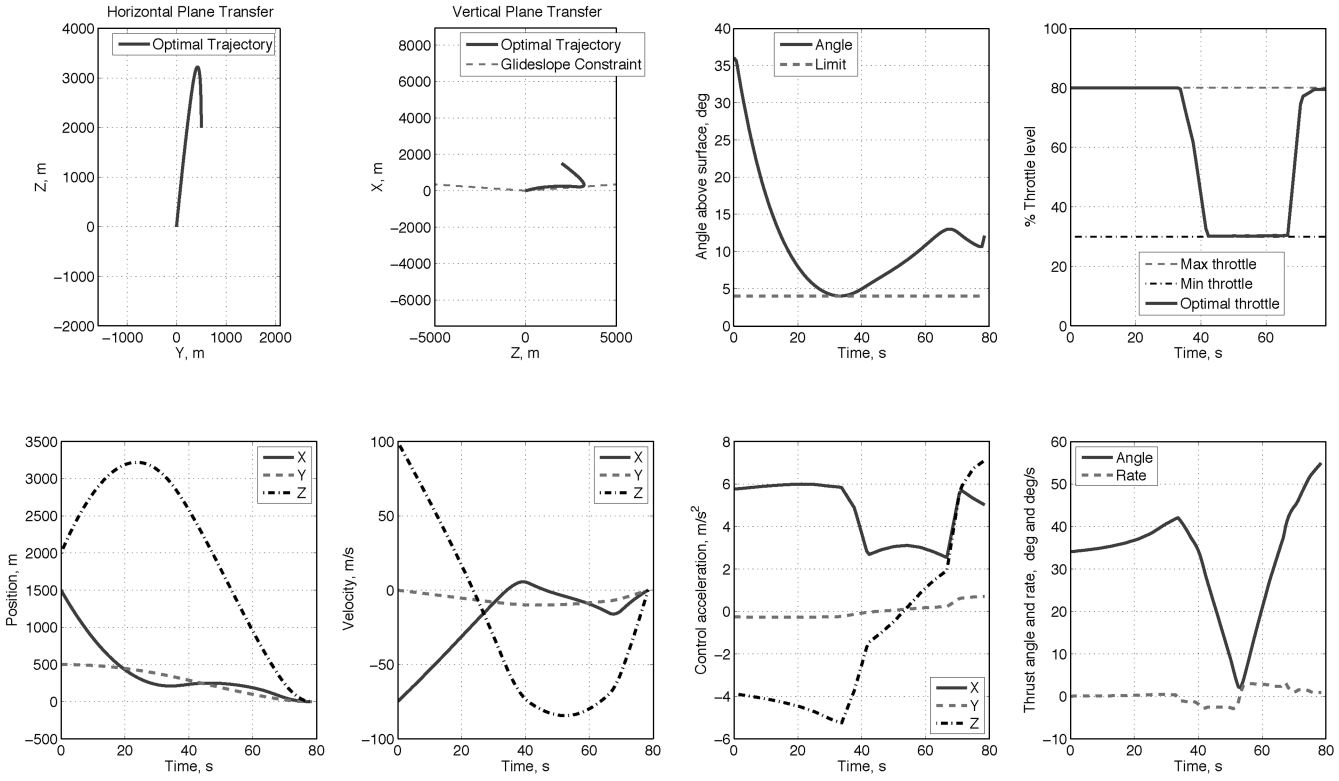

Fig. 2 Results of minimum-landing-error targeting approach for case 1 with $\mathbf{r_0} = [1500 \text{ m} \quad 500 \text{ m} \quad 2000 \text{ m}]^T$ and $\dot{\mathbf{r}}_0 = [-75 \text{ m/s} \quad 0 \quad 100 \text{ m/s}]^T$. In this case, a feasible solution to the target exists, so the prioritized minimum-landing-error algorithm returns the minimum-fuel solution to the target.

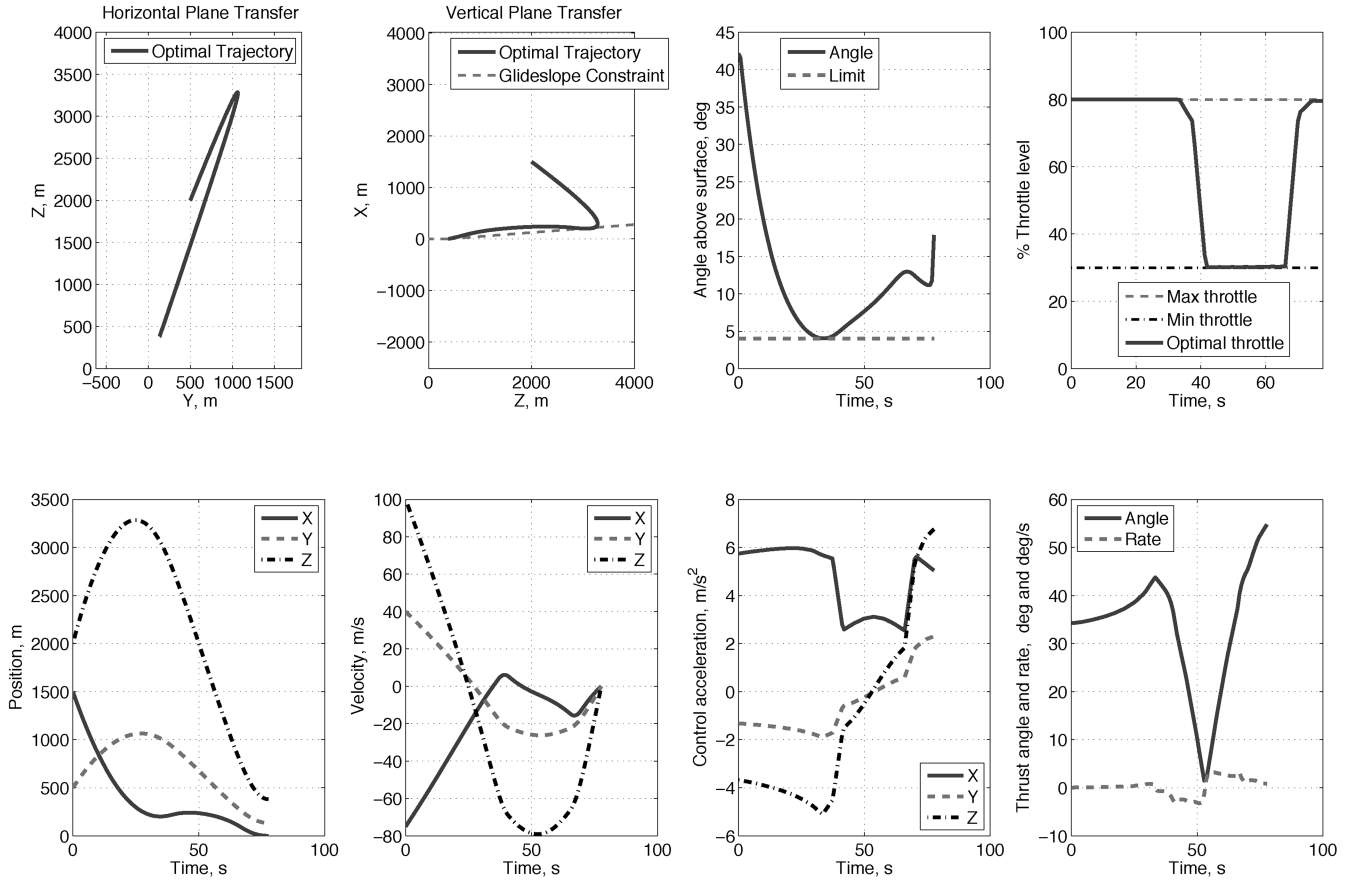

Fig. 3 Results of minimum-landing-error targeting approach for case 2 with $\mathbf{r}_0 = [1500\ \text{m} \quad 500\ \text{m} \quad 2000\ \text{m}]^T$ and $\dot{\mathbf{r}}_0 = [-75\ \text{m/s} \quad 40\ \text{m/s} \quad 100\ \text{m/s}]^T$. In this case, no feasible solution to the target exists, so the minimum-landing-error algorithm approach returns the solution that minimizes the final distance to the target. Notice that the final altitude is zero and velocity are zero, indicating that safe landing is achieved. The final position is 404 m from the original target.

available fuel. The total computation time required was 14.74 s, and 23 iterations of golden search were used.

B. Unimodality of Cost as a Function of Time of Flight

In this section, we empirically demonstrate that the optimal cost of the minimum-landing-error solution is unimodal in the time of flight. Throughout this section, we use the spacecraft parameters given in Eq. (72). Figure 4 shows $J(t_f)$ for a typical set of initial conditions. The graph was generated by specifying t_f in increments of 1 s and solving Problem 7 for each value of t_f. In this case, $J(t_f)$ is unimodal, as required. By reducing the time increments to 0.01 s close to the minimum, the optimum was found to be at $t_f = 56.35$ s. The golden search determines the optimum to be 55.83 s, which is an error of only 0.9%. Again, golden search was terminated when the optimal time of flight was known to within an interval of 3.0 s. The efficacy of the golden search approach was investigated for a range of initial conditions by calculating the error between t_f^* determined through golden search and the true optimum. The true optimum was determined approximately by calculating $J(t_f)$ for $t_f \in [30, 150]$ in increments of 1 s. Initial conditions were selected at random using a uniform distribution across a box of values specified by

$$\begin{bmatrix} 1\ \text{km} \\ -5\ \text{km} \\ -5\ \text{km} \end{bmatrix} \leq \mathbf{r}_0 \leq \begin{bmatrix} 2\ \text{km} \\ 5\ \text{km} \\ 5\ \text{km} \end{bmatrix}$$
$$\begin{bmatrix} -30\ \text{m/s} \\ -100\ \text{m/s} \\ -100\ \text{m/s} \end{bmatrix} \leq \dot{\mathbf{r}}_0 \leq \begin{bmatrix} -10\ \text{m/s} \\ 100\ \text{m/s} \\ 100\ \text{m/s} \end{bmatrix} \tag{76}$$

Since we are only concerned with the unimodality of $J(t_f)$ in the minimum-landing-error case, solutions for which a feasible trajectory to the target existed were discarded. One hundred random initial conditions were chosen, and for these the average percentage error in t_f^* was 0.012% with a standard deviation of 0.057%. The maximum error across all instances was 1.8%. This demonstrates that the golden search approach is effective for a broad range of initial conditions in the case of minimum-landing-error powered-descent guidance.

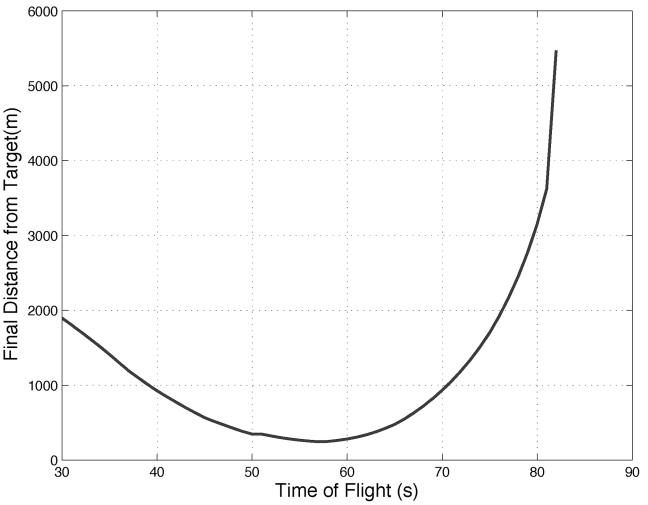

Fig. 4 Dependence of minimum distance from target on time of flight for a typical set of initial conditions. The relationship is unimodal and has an optimum at 56.35 s. The golden search determines the optimum to be 55.83 s, which is an error of only 0.9%.

VI. Conclusions

In this paper, we have presented a new approach for optimal powered-descent guidance that minimizes the final distance of the lander to the target for a given amount of fuel. If a feasible trajectory to the target exists, the new algorithm returns the minimum-fuel solution that reaches the target. The new approach uses a new analytic convexification result to pose the guidance problem as a second-order cone program, which can be solved to global optimality with a priori known bounds on the number of iterations required. Furthermore, the new approach can handle maximum and minimum thrust-magnitude constraints explicitly as well as a glide-slope constraint. The algorithm was demonstrated in simulation with a Mars landing example.

Appendix: Review and Extension of Technical Results on Convexification

In this Appendix the key technical lemma, Lemma 1, from [3] is restated and extended. Omitted in [3] was that the conclusions of Lemma 1 are valid only when the optimal state trajectory of the relaxed problem remains in the interior of the set of feasible states. It has been empirically noted that solutions to the powered-descent guidance problem can momentarily intersect the boundary of the set of feasible states in some cases. Here, we extend Lemma 1 to be valid when this is the case. The restatement of Lemma 1 of [3] follows:

Lemma 4. Consider a solution of Problem 2 given by $\{t_f^*, T_c^*(\cdot), \Gamma^*(\cdot)\}$ such that the corresponding state trajectory satisfies $\mathbf{r}^*(t) \in \text{int}\mathbf{X}\ \forall\ t \in (0, t_f^*)$. Then $\{t_f^*, T_c^*(\cdot)\}$ is also a solution of Problem 1 and $\|T_c^*(t)\| = \rho_1$ or $\|T_c^*(t)\| = \rho_2$ for $t \in [0, t_f^*]$.

Proof: We use a.e. to mean almost everywhere: that is, everywhere except on a set of measure zero. The Hamiltonian for Problem 2 is given by [23,24]

$$H(\mathbf{x}, T_c, \Gamma, \lambda_0, \lambda) = \lambda_0\Gamma + \lambda_1^T\dot{\mathbf{r}} + \frac{\lambda_2^T T_c}{m} + \lambda_2^T g - \alpha\lambda_3\Gamma \quad \text{(A1)}$$

where $\mathbf{x} \triangleq (\mathbf{r}, \dot{\mathbf{r}}, m)$ is the state vector, $\lambda_0 \le 0$, $\lambda = (\lambda_1, \lambda_2, \lambda_3)$ is the costate vector with $\lambda_{1,2} \in \mathbb{R}^3$, and $\lambda_3 \in \mathbb{R}$. We first state a general form of necessary conditions of optimality given on page 186 of [23] (*Pontryagin's maximum principle*). To do that, define a vector $\mathbf{v} \triangleq (T_c, \Gamma)$. Since the set defined by control constraints,

$$\Psi = \{(T_c, \Gamma) \in \mathbb{R}^4 \colon \|T_c\| \le \Gamma, \rho_1 \le \Gamma \le \rho_2\}$$

is a fixed set, any optimal solution defined by the pair $(\mathbf{x}^*, \mathbf{v}^*)$ on $[0, t_f^*]$ must satisfy the following: There exist a $\lambda_0 \le 0$ and an absolutely continuous vector function $\lambda \in \mathbb{R}^7$ such that

1) $(\lambda_0, \lambda(t)) \ne 0\ \forall\ t \in [0, t_f^*]$ and

$$\dot{\lambda} = -\frac{\partial H}{\partial \mathbf{x}}(\mathbf{x}^*, \mathbf{v}^*, \lambda_0, \lambda) \quad \text{(A2)}$$

2) The *pointwise maximum principle* given below must be satisfied, where a.e. on $[0, t_f]$ means that the condition is valid on a set of points in the interval, with an exception of a set of points with measure zero [25]:

$$H(\mathbf{x}^*(t), \mathbf{v}^*(t), \lambda_0, \lambda) \ge H(\mathbf{x}^*(t), \mathbf{v}, \lambda_0, \lambda) \quad \forall\ \mathbf{v} \in \Psi \quad \text{a.e. on } t \in [0, t_f^*] \quad \text{(A3)}$$

3) The following *transversality condition* must be satisfied: Let $\psi \triangleq (\mathbf{x}^*, \mathbf{v}^*, \lambda_0, \lambda)$, then the vector $(H(\psi(0)), -\lambda(0), -H(\psi(t_f^*)), \lambda(t_f^*))$ must be orthogonal to the manifold formed by the set of vectors $(0, \mathbf{x}^*(0), t_f^*, \mathbf{x}^*(t_f^*))$ defining the initial and final conditions.

The first necessary condition (A2) implies that by using $\lambda = (\lambda_1, \lambda_2, \lambda_3)$, where $\lambda_{1,2} \in \mathbb{R}^3$ and $\lambda_3 \in \mathbb{R}$,

$$\dot{\lambda}_1 = 0 \quad \text{(A4)}$$

$$\dot{\lambda}_2 = -\lambda_1 \quad \text{(A5)}$$

$$\dot{\lambda}_3 = \frac{1}{m^2}\lambda_2^T T_c^*$$

Note that the transversality condition with the specified end conditions on the position and velocity vectors at $t = 0$ and t_f^* of this problem imply that

$$\lambda_3(t_f^*) = 0, \qquad H(\psi(t_f^*)) = 0$$

This follows from the fact that the tangent plane for the manifold of end conditions is spanned by two unit vectors $\mathbf{e}_6$ and $\mathbf{e}_{14}$. Hence, the inner product of $\mathbf{e}_6$ and $\mathbf{e}_{14}$ with $(H(\psi(0)), -\lambda(0), -H(\psi(t_f^*)), \lambda(t_f^*))$ must be zero.

Now we show by contradiction that $\lambda_2(t) = 0\ \forall\ t \in [0, t_f^*]$ is not possible. Since λ_1 is constant and $\lambda_3(t_f^*) = 0$, if $\lambda_2 = 0$, then $\lambda_1 = 0$, as well as $\lambda_3 = 0$. Since $H(\psi(t_f^*)) = 0$, this implies that $\lambda_0 = 0$. This violates the first necessary condition for optimality because it leads to $(\lambda_0, \lambda(t)) = 0\ \forall\ t \in [0, t_f^*]$. Consequently, $\lambda_2(t) = 0\ \forall\ t \in [0, t_f^*]$ does not hold. This implies $\lambda_2(t) = -\lambda_1 t + a$ for some constant a. Since λ_2 is not identically zero, it can be zero, at most, at one point on $[0, t_f^*]$. We can express the Hamiltonian as

$$H(\mathbf{x}(t), T_c, \Gamma, \lambda_0, \lambda(t)) = R_1(t)\Gamma + R_2(t)^T T_c + R_0(t) \quad \text{(A6)}$$

where:

$$R_0(t) = \lambda_1(t)^T\dot{\mathbf{r}}(t) + \lambda_2(t)^T g, \qquad R_1(t) = \lambda_0 - \alpha\lambda_3(t)$$
$$R_2(t) = \frac{\lambda_2(t)}{m(t)}$$

Since we know that $\lambda_2(t) \ne 0$ a.e. on $[0, t_f^*]$, $m^*(t) > 0$, and H depends linearly on T_c, the pointwise maximum principle given by Eq. (A3) implies that the Hamiltonian is maximized at the boundary of the set Ψ; that is, we have the following for the optimal solution:

$$\|T_c^*(t)\| = \Gamma^*(t), \quad \text{a.e. on } [0, t_f^*] \quad \text{(A7)}$$

Note that we use Theorem 3.1 in [26], which states that the maximum of a nonconstant convex function on a convex domain occurs at the boundary of the domain, to draw the above conclusion. This also implies that

$$\rho_1 \le \|T_c^*(t)\| \le \rho_2, \quad \text{a.e. on } [0, t_f^*]$$

See [3] for the remainder of the proof. □

The difference between the statement of Lemma 1 in [3] and Lemma 4 is that Lemma 1 did not include the condition that the optimal trajectory of Problem 2 is in the interior of the set of feasible states. This condition must be included for the form of the maximum principle used to be applicable. Another minor extension from [3] is that the final position and velocity in Problems 1 and 2 now have arbitrary user-specified values. This extension is possible since the proof of the result relies only on the fact that the end position and velocity are fixed and not the specific values to which they are fixed.

Lemma 5. If an optimal solution of Problem 2 has the property that

$$\Gamma^*(t) = \|T_c^*(t)\| \quad \forall\ t \in [0, t_f^*] \quad \text{(A8)}$$

then this solution is also optimal for Problem 1.

Proof: To prove this claim, first observe that Problem 2 with the additional constraint $\Gamma(t) = \|T_c(t)\|$ for $t \in [0, t_f]$ is identical to Problem 1. Hence, an optimal solution to Problem 2 that satisfies the condition (A8) is also feasible for Problem 1 and hence has cost greater than or equal to the optimal cost of Problem 1. Since Problem 2 is a relaxation of Problem 1, any optimal solution to Problem 2 has cost less than or equal to the optimal cost of Problem 1. Hence, the cost of the optimal solution to Problem 2 is equal to the optimal cost of Problem 1 from which the result follows.

Lemma 4 can be seen as a result that establishes that the condition (A8) is always satisfied for optimal solutions to Problem 2 with $\mathbf{r}^*(t) \in \text{int}\mathbf{X}$ for $t \in (0, t_f^*)$, in which case Lemma 5 enables us to declare that the optimal solution of Problem 2 is an optimal

solution of Problem 1. In this case, a lossless convexification of Problem 1 is achieved via Problem 2. Our next result presents an extended result that establishes that condition (A8) is also satisfied for trajectories that touch the boundary of $\mathbf{X}$. This extension is nontrivial, since having contact with the boundary of the feasible set of states can lead to discontinuities in the costate vector, whose behavior is critical in proving the lossless convexification of the guidance problem. Before we state our next result, we observe that the set $\mathbf{X}$ satisfies the following conditions for $h(\mathbf{r}) := \|S(\mathbf{r}-\mathbf{s})\| - \mathbf{c}^T(\mathbf{r}-\mathbf{s})$, $\partial\mathbf{X} = \{\mathbf{r} \in \mathbb{R}^3 \colon h(\mathbf{r}) = 0\}$ and for all $\mathbf{r} \in \partial\mathbf{X}$ such that $\mathbf{r} \neq \mathbf{s}$:

$$\frac{\partial h}{\partial \mathbf{r}}(\mathbf{r}) \neq 0 \quad \text{and} \quad \exists\, \mathbf{u}, \qquad \|\mathbf{u}\| = 1, \qquad \text{subject to } \mathbf{u}^T \frac{\partial h}{\partial \mathbf{r}}(\mathbf{r}) = 0$$
$$\mathbf{u}^T(\mathbf{r}-\mathbf{s}) > 0, \qquad \mathbf{u}^T\mathbf{g} \leq 0 \tag{A9}$$

where $\mathbf{s}$ is the target location such that $\mathbf{e}_1^T\mathbf{s} = 0$ and $[\,\mathbf{e}_2 \quad \mathbf{e}_3\,]^T\mathbf{s} = \mathbf{q}$. These conditions are straightforward to verify geometrically for $\mathbf{X}$.

Lemma 6. Consider a solution of Problem 2 given by $\{t_f^*, T_c^*(\cdot), \Gamma^*(\cdot)\}$ and the corresponding state trajectory $\mathbf{r}^*(\cdot)$. If $\mathbf{r}^*(t) \in \partial\mathbf{X}$ for, at most, one point $t \in (0, t_f^*)$, then $T_c^*(\cdot)$ is also an optimal solution of Problem 1 and $\|T_c^*(t)\| = \rho_1$ or $\|T_c^*(t)\| = \rho_2$ almost everywhere $t \in [0, t_f^*]$.

Proof: From Lemma 4 we know that if $\mathbf{r}^*(t)$ is never in $\partial\mathbf{X}$ for $t \in (0, t_f^*)$ then $T_c^*(\cdot)$ is also an optimal solution of Problem 1 and $\|T_c^*(t)\| = \rho_1$ or $\|T_c^*(t)\| = \rho_2$ almost everywhere $t \in [0, t_f^*]$. We need consider only the case when $\mathbf{r}^*(t) \in \partial\mathbf{X}$ for a single instant $t_m \in (0, t_f^*)$. Since the condition (A9) holds, Theorem 24 in [27] (Note 1 on page 292) states that the maximum principle (A3) holds in the interior of $\mathbf{X}$ and the following *jump condition* on the costate vector holds for some $\mu \geq 0$:

$$\lambda(t_m^+) = \lambda(t_m^-) + \mu \begin{bmatrix} \frac{\partial h}{\partial \mathbf{r}}(\mathbf{r}(t_m)) \\ \mathbf{0} \\ 0 \end{bmatrix} \tag{A10}$$

where we have used the fact that h only depends on $\mathbf{r}$, the position vector. The above jump condition implies that

$$\lambda_1(t_m^+) = \lambda_1(t_m^-) + \mu \frac{\partial h}{\partial \mathbf{r}}(\mathbf{r}(t_m)), \qquad \lambda_2(t_m^+) = \lambda_2(t_m^-)$$
$$\lambda_3(t_m^+) = \lambda_3(t_m^-) \tag{A11}$$

Now we will show that $\lambda_2(t) \neq 0$ a.e. on $[0, t_f^*]$ to complete the proof via the pointwise maximum principle (A3). First note that the portion of the optimal solution $\{\mathbf{T}_c^*(\cdot), \Gamma^*(\cdot)\}$ on $[t_m, t_f^*]$ is an optimal solution of Problem 2 for the initial conditions $\mathbf{r}(0) = \mathbf{r}^*(t_m)$, $\dot{\mathbf{r}}(0) = \dot{\mathbf{r}}^*(t_m)$, and $m(0) = m^*(t_m)$. This can be shown via a proof by contradiction. Suppose this statement is not true, then there is an optimal solution with a trajectory $\{t_f^{**}, \mathbf{T}_c^{**}(\cdot), \Gamma^{**}(\cdot)\}$ for the above initial conditions with a lesser fuel cost. Hence, the following solution will be a feasible solution of Problem 2 for the initial conditions $\mathbf{r}(0) = \mathbf{r}_0$, $\dot{\mathbf{r}}(0) = \dot{\mathbf{r}}_0$, and $m(0) = m_{\text{wet}}$ with a lesser fuel cost, which is a contradiction:

$$\{T_c(t), \Gamma(t)\} = \begin{cases} \{T_c^*(t), \Gamma^*(t)\} & \text{for } t \in [0, t_m) \\ \{T_c^{**}(t - t_m), \Gamma^{**}(t - t_m)\} & \text{for } t \in [t_m, t_m + t_f^{**}] \end{cases}$$

From the proof of Lemma 4, the optimality of this portion of the trajectory (after the instant of contact t_m) indicates that $\lambda_2(t) \neq 0$ a.e. on $[t_m, t_f^*]$. From Eqs. (A5) and (A10) we have

$$\lambda_2(t) = -\lambda_1(0)t + \lambda_2(0) \qquad t \in [0, t_m]$$
$$\lambda_2(t) = -\lambda_1(t_m^+)(t - t_m) + \lambda_2(t_m) \qquad t \in [t_m, t_f^*] \tag{A12}$$

Suppose $\lambda_2(t_m) \neq 0$ then, since λ_2 is a linear function of time over $[0, t_m]$, $\lambda_2(t) \neq 0$ a.e. on $[0, t_m]$. This implies that $\lambda_2(t) \neq 0$ a.e. on $[0, t_f^*]$, and the result follows in an identical manner to the proof of Lemma 4. Therefore, we only need to consider the case when $\lambda_2(t_m) = 0$. Let $\zeta \triangleq (\partial h/\partial \mathbf{r})(\mathbf{r}^*(t_m))$. First consider the case when $\mathbf{r}^*(t_m) \neq \mathbf{s}$. In this case, there exists a unit vector $\mathbf{u}$ satisfying Eq. (A9). Since $\mathbf{r}^*(t_f^*) = \mathbf{s}$ and $\mathbf{u}^T(\mathbf{r}^*(t_m) - \mathbf{s}) > 0$, there exists some interval $(t_1, t_2) \subset [t_m, t_f^*]$ such that $v_u(t) \triangleq \mathbf{u}^T\dot{\mathbf{r}}^*(t) < 0$ on (t_1, t_2) and $t_2 - t > 0$. Since $\ddot{\mathbf{r}}(t) = \mathbf{g} + [T_c(t)/m(t)]$, $\mathbf{u}^T\mathbf{g} < 0$, and $v_u(t) < 0$ over an interval, there must be a control force acting along $\mathbf{u}$ over a period of time to have $\mathbf{u}^T\dot{\mathbf{r}}(t_f^*) = 0$: that is, $\mathbf{u}^T T_c^*(t) > 0$ for $t \in (t_3, t_4) \subset [t_m, t_f^*]$ for some $t_4 - t_3 > 0$. Having $\lambda_2 \neq 0$ in (t_3, t_4) and the pointwise maximum principle (A3) imply that maximizing the Hamiltonian when $\lambda_2(t) \neq 0$ requires the following condition to hold:

$$T_c^*(t) = \Gamma^*(t) \frac{\lambda_2(t)}{\|\lambda_2(t)\|} \tag{A13}$$

which also implies that $\mathbf{u}^T\lambda_2(t) > 0$ on this subinterval. Since $\lambda_2(t) = -(\lambda_1(t_m^-) + \mu\zeta)(t - t_m)$, this implies that (note that $\mathbf{u}^T\zeta = 0$)

$$\mathbf{u}^T\lambda_2(t) = -\mathbf{u}^T\lambda_1(t_m^-)(t - t_m) + \mu\mathbf{u}^T\zeta(t - t_m)$$
$$= -\mathbf{u}^T\lambda_1(t_m^-)(t - t_m)$$

Since $\mathbf{u}^T\lambda_2(t) > 0$ on some nonzero length subinterval of (t_3, t_4), where $t - t_m > 0$, this implies that $\mathbf{u}^T\lambda_1(t_m^-) \neq 0$, which then implies that $\lambda_1(t_m^-) = \lambda_1(0) \neq 0$. Then by using Eq. (A12) $\{\lambda_2$ is a linear function of time on $[0, t_m]$ with $\lambda_1(0) \neq 0\}$, we obtain $\lambda_2(t) \neq 0$ a.e. on $[0, t_m]$ as well as $[t_m, t_f^*]$ {that is, $\lambda_2(t) \neq 0$ a.e. on $[0, t_f^*]$}, and the result follows in an identical manner to the proof of Lemma 4.

Next we consider the case when $\mathbf{r}^*(t_m) = \mathbf{s}$. In this case, we will show that $\dot{\mathbf{r}}^*(t_m) = \mathbf{0}$ and hence the maneuver is over: i.e., $t_m = t_f^*$. First note that $\mathbf{n}^T\dot{\mathbf{r}}^*(t_m) = 0$, where $\mathbf{n} \triangleq \mathbf{c}/\|\mathbf{c}\|$. This follows from the fact that $\mathbf{n}^T(\mathbf{r}^*(t) - \mathbf{s}) \geq 0$ for $t \leq t_m$, and since $\mathbf{n}^T(\mathbf{r}^*(t_m) - \mathbf{s}) = 0$, this implies that $\mathbf{n}^T\dot{\mathbf{r}}^*(t) \leq 0$ for $t \in [t_m - b, t_m]$ for some $b > 0$. Now if $\mathbf{n}^T\dot{\mathbf{r}}^*(t_m) < 0$, then $\mathbf{n}^T(\mathbf{r}^*(t) - \mathbf{s}) < 0$ for some $t \in (t_m, t_m + a)$, where $a > 0$, which violates the state constraint. Hence, $\mathbf{n}^T\dot{\mathbf{r}}^*(t_m) = \mathbf{0}$. Now we will show by contradiction that for any unit vector $\mathbf{e}$ such that $\mathbf{e}^T\mathbf{n} = 0$, we have $v_e \triangleq \mathbf{e}^T\dot{\mathbf{r}}^*(t_m) = 0$. First let us assume that there exists a unit vector $\mathbf{e}$ such that $\mathbf{e}^T\mathbf{n} = 0$ and $v_e > 0$. Let $\alpha > 0$ be the maximum possible magnitude of acceleration due to the gravity and the thrust vector along any direction. Then

$$0 \leq r_c(t) \triangleq \mathbf{c}^T(\mathbf{r}^*(t) - \mathbf{s}) = \|\mathbf{c}\|\mathbf{n}^T(\mathbf{r}^*(t) - \mathbf{s}) \leq \alpha\|\mathbf{c}\|\tau^2/2$$

where $\tau = t - t_m$ and we have used the fact that $\mathbf{n}^T\dot{\mathbf{r}}^T(t_m) = 0$. Also define

$$r_e(t) \triangleq \mathbf{e}^T(\mathbf{r}^*(t) - \mathbf{s}) \geq v_e\tau - \alpha\tau^2/2$$

Then

$$r_e(\tau) - r_c(\tau) \geq v_e\tau - \alpha(1 + \|\mathbf{c}\|)\tau^2/2$$
$$= v_e\tau(1 - \alpha(1 + \|\mathbf{c}\|)\tau/(2v_e))$$

Now note that $r_e(\tau) - r_n(\tau) > 0$ for $\tau \in [0, (2v_e)/(\alpha(1 + \|\mathbf{c}\|)))$ and that $h(\mathbf{r}^*(\tau)) \geq r_e(\tau) - r_c(\tau)$ since $\|S(\mathbf{r} - \mathbf{s})\| \geq \|\mathbf{e}^T(\mathbf{r} - \mathbf{s})\|$. Since $r_e(\tau) - r_c(\tau) > 0$, this means that $\mathbf{r}^*(\tau) \notin \mathbf{X}$ for $\tau \in [0, [0, (2v_e)/(\alpha(1 + \|\mathbf{c}\|)))]$, which is a contradiction. Hence, there exists no direction with a unit vector $\mathbf{e}$, such that $v_e > 0$, which also holds true for $\pm\mathbf{n}$, which implies that $\dot{\mathbf{r}}^*(t_m) = 0$. Then at time t_m, the position is at the target and the velocity is zero. Hence, t_m is the optimal time of flight t_f^*. Hence, $\mathbf{r}^*(t_f) \in \text{int}\mathbf{X}\ \forall\ t \in (0, t_f^*)$ and from Lemma 4 the result follows.

In summary, if we compute an optimal solution of the convex Problem 2 via the algorithm in [3] and obtain a state trajectory that touches the boundary of the set of feasible states, at most, once during the maneuver before reaching its target, this solution is also *optimal* for the nonconvex Problem 1.

For Mars landing, all of the solutions we have generated via the algorithm of [3] have touched the boundary, at most, once. Hence, they satisfy Lemma 6 for lossless relaxation, and so they are optimal solutions to the original nonconvex optimal control problem for Mars powered-descent guidance. The solutions generated include an extensive empirical investigation across the space of feasible initial conditions and system parameters.

However, through careful selection of the problem parameters, cases can be constructed such that an optimal solution of Problem 2 lies on the boundary for a nonzero duration. Even in these cases, we observe that the optimal trajectories obtained by solving Problem 2 satisfy the control constraints of Problem 1. The theoretical analysis of such trajectories requires a different version of the maximum principle (see Theorem 25 on page 292 in [27]) from the one used herein. Since this additional step uses substantially more complex analyses and these trajectories are rarely encountered in practice, it is not considered here.

Acknowledgment

This research was performed at the Jet Propulsion Laboratory, California Institute of Technology, under a contract with NASA.

References

[1] Williams, D. R., "Mars Pathfinder Landing Site," Dec. 2004, http://nssdc.gsfc.nasa.gov/planetary/marsland.html [retrieved 22 March 2010].

[2] Knocke, P. C., Wawrzyniak, G. G., Kennedy, B. M., Desai, P. N., Parker, T. J., Golombek, M. P., Duxbury, T. C., and Kass, D. M., "Mars Exploration Rovers Landing Dispersion Analysis," Proceedings of the AIAA/AAS Astrodynamics Specialist Conference, AIAA Paper 2004-5093, 2004.

[3] Acikmese, B., and Ploen, S. R., "Convex Programming Approach to Powered Descent Guidance for Mars Landing," *Journal of Guidance, Control, and Dynamics*, Vol. 30, No. 5, 2007, pp. 1353–1366. doi:10.2514/1.27553

[4] Arvidson, R., Adams, D., Bonglio, G., Christensen, P., Cull, S., Golombek, M., et al., "Mars Exploration Program 2007 Phoenix Landing Site Selection and Characteristics," *Journal of Geophysical Research*, Vol. 113, 2008, Paper E00A03. doi:10.1029/2007JE003021

[5] Wolf, A. A., Tooley, J., Ploen, S., Ivanov, M., Acikmese, B., and Gromov, K., "Performance Trades for Mars Pinpoint Landing," IEEE Aerospace Conference, Inst. of Electrical and Electronics Engineers Paper 1661, 2006.

[6] Meditch, J. S., "On the Problem of Optimal Thrust Programming for a Lunar Soft Landing," *IEEE Transactions on Automatic Control*, Vol. 9, No. 4, 1964, pp. 477–484. doi:10.1109/TAC.1964.1105758

[7] Miele, A., *The Calculus of Variations in Applied Aerodynamics and Flight Mechanics in Optimization Techniques*, edited by G. Leitmann, Academic Press, New York, 1962.

[8] Klumpp, A. R., "Apollo Lunar Descent Guidance," *Automatica*, Vol. 10, No. 2, 1974, pp. 133–146. doi:10.1016/0005-1098(74)90019-3

[9] Topcu, U., Casoliva, J., and Mease, K., "Fuel Efficient Powered Descent Guidance for Mars Landing," AIAA Paper 2005-6286, 2005.

[10] Sostaric, R., and Rea, J., "Powered-Descent Guidance Methods for the Moon and Mars," AIAA Guidance, Navigation, and Control Conference, San Francisco, AIAA Paper 2005-6287, 2005.

[11] Najson, F., and Mease, K., "A Computationally Non-Expensive Guidance Algorithm for Fuel Efficient Soft Landing," AIAA Guidance, Navigation, and Control Conference, San Francisco, AIAA Paper 2005-6289, 2005.

[12] Steinfeldt, B., Grant, M., Matz, D., and Braun, R., "Guidance, Navigation, and Control Technology System Trades for Mars Pinpoint Landing," AIAA Guidance, Navigation, and Control Conference, AIAA Paper 2008-6216, 2008.

[13] Ye, Y., *Interior Point Algorithms*, Wiley, New York, 1997.

[14] Sturm, J. F., "Using SeDuMi 1.02, a MATLAB Toolbox for Optimization over Symmetric Cones," *Optimization Methods and Software*, Vol. 11, No. 1, 1999, pp. 625–653. doi:10.1080/10556789908805766

[15] Sturm, J. F., "Implementation of Interior Point Methods for Mixed Semidefinite and Second Order Cone Optimization Problems," *Optimization methods and software*, Vol. 17, No. 6, 2002, pp. 1105–1154. doi:10.1080/1055678021000045123

[16] Boyd, S., and Vandenberghe, L., *Convex Optimization*, Cambridge Univ. Press, New York, 2004.

[17] D'Souza, C., "An Optimal Guidance Law for Planetary Landing," AIAA Guidance, Navigation, and Control Conference, AIAA Paper 1997-3709, 1997.

[18] Ploen, S., Acikmese, B., and Wolf, A., "A Comparison of Powered Descent Guidance Laws for Mars Pinpoint Landing," AIAA Guidance, Navigation, and Control Conference, Keystone, CO, AIAA Paper 2006-6676, 2006.

[19] Antsaklis, P. J., and Michel, A. N., *A Linear Systems Primer*, Birkhäuser, Boston, 2007.

[20] Vandenberghe, L., and Boyd, S., "Semidefinite Programming," *SIAM Review*, Vol. 38, No. 1, 1996, pp. 49–95. doi:10.1137/1038003

[21] Acikmese, B., Blackmore, L., Scharf, D. P., and Wolf, A., "Enhancements on the Convex Programming Based powered-descent Guidance Algorithm for Mars Landing," AIAA Guidance, Navigation, and Control Conference, AIAA Paper 2008-6426, 2008.

[22] Bertsekas D. P., *Nonlinear Programming*, 2nd ed., Athena Scientific, Belmont, MA, 2000.

[23] Berkovitz, L. D., *Optimal Control Theory*, Springer–Verlag, New York, 1975.

[24] Macki, J., and Strauss, A., *Introduction to Optimal Control Theory*, Springer–Verlag, New York, 1982.

[25] Bartle, R. G., *The Elements of Integration and Lebesgue Measure*, Wiley, New York, 1985.

[26] Berkovitz, L. D., *Convexity and Optimization in* $\mathbb{R}^n$, Wiley, New York, 2002.

[27] Pontryagin, L. S., Boltyanskii, V. G., Gamkrelidze, R. V., and Mischenko, E. F., *The Mathematical Theory of Optimal Processes*, Pergamon, New York, 1964.